2022

# Greater loss and fragmentation of savannas than forests over the last three decades in Yunnan Province, China

R Sedricke Lapuz

Angelica Kristina M. Jaojoco

Sheryl Rose C. Reyes

Jose Don T. De Alban

Kyle W. Tomlinson

ENVIRONMENTAL RESEARCH
LETTERS

LETTER • OPEN ACCESS

# Greater loss and fragmentation of savannas than forests over the last three decades in Yunnan Province, China

To cite this article: R Sedricke Lapuz *et al* 2022 *Environ. Res. Lett.* **17** 014003

ENVIRONMENTAL RESEARCH
LETTERS

OPEN ACCESS

RECEIVED
14 July 2021

REVISED
14 October 2021

ACCEPTED FOR PUBLICATION
17 November 2021

PUBLISHED
21 December 2021



LETTER

# Greater loss and fragmentation of savannas than forests over the last three decades in Yunnan Province, China

**R Sedricke Lapuz[1,2], Angelica Kristina M Jaojoco[3], Sheryl Rose C Reyes[4,5], Jose Don T De Alban[6] and Kyle W Tomlinson[1,7,*]**

[1] Center for Integrative Conservation, Xishuangbanna Tropical Botanical Garden, Chinese Academy of Sciences, Menglun, Yunnan 666303, People's Republic of China
[2] University of Chinese Academy of Sciences, No. 19A Yuquan Road, Beijing 10049, People's Republic of China
[3] PS241 Consulting Inc., City of San Pedro, Laguna 4023, Philippines
[4] United Nations University—Institute for the Advanced Study of Sustainability, 5-53-70 Jingumae, Shibuya-ku, Tokyo 150-8925, Japan
[5] Geomatics for Environment and Development Laboratory, Manila Observatory, Ateneo de Manila University Campus, Loyola Heights, Quezon City 1101, Philippines
[6] Department of Biological Sciences, National University of Singapore, Singapore 117543, Singapore
[7] Center of Conservation Biology, Core Botanical Gardens, Chinese Academy of Sciences, Menglun, Yunnan 666303, People's Republic of China
[*] Author to whom any correspondence should be addressed.

**E-mail:** kyle.tomlinson@xtbg.org.cn

**Keywords:** climate-vegetation interactions, fire, fragmentation, hybrid classification, Landsat, land-use change, woody encroachment

Supplementary material for this article is available online

## Abstract

Yunnan Province, southwest China, has a monsoonal climate suitable for a mix of fire-driven savannas and fire-averse forests as alternate stable states, and has vast areas with savanna physiognomy. Presently, savannas are only formally recognised in the dry valleys of the region, and a no-fire policy has been enforced nationwide since the 1980s. Misidentification of savannas as forests may have contributed to their low protection level and fire-suppression may be contributing to vegetation change towards forest states through woody encroachment. Here, we present an analysis of vegetation and land-use change in Yunnan for years 1986, 1996, 2006, and 2016 by classifying Landsat imagery using a hybrid of unsupervised and supervised classification. We assessed how much savanna area had changed over the 3 decades (area loss, fragmentation), and of this how much was due to direct human intervention versus vegetation transition. We also assessed how climate (mean annual temperature, aridity), landscape accessibility (slope, distance to roads), and fire had altered transition rates. Our classification yielded accuracy values of 77.89%, 82.16%, 94.93%, and 86.84% for our four maps, respectively. In 1986, savannas had the greatest area of any vegetation type in Yunnan at 40.30%, whereas forest cover was 30.78%. Savanna coverage declined across the decades mainly due to a drop in open parkland savannas, while forest cover remained stable. Savannas experienced greater fragmentation than forests. Savannas suffered direct loss of coverage to human uses and to woody encroachment. Savannas in more humid environments switched to denser vegetation at a higher rate. Fire slowed the rate of conversion away from savanna states and promoted conversion towards them. We identified remaining savannas in Yunnan that can be considered when drafting future protected areas. Our results can inform more inclusive policy-making that considers Yunnan's forests and savannas as distinct vegetation types with different management needs.

## 1. Introduction

Savannas are ecosystems characterized by a ground layer dominated by grasses and an open canopy of trees that allows direct sun to penetrate to the understory (Scholes and Archer 1997). Competition between trees and grasses asymmetrically favours trees, therefore, savannas are dependent on disturbance to remove tree biomass and open up canopies, either by fire (Higgins *et al* 2000), herbivory (Sankaran *et al* 2013), or drought (Fensham *et al* 2009). In Asia, savannas are extensively found across the drier parts of the monsoonal belt of its tropical and subtropical regions (Ratnam *et al* 2016). Fossil and molecular evidence indicate that savannas and their associated species have been widely present in the region since at least the early Pleistocene (Shen *et al* 2009, Edwards *et al* 2010, Zhang *et al* 2011, Ratnam *et al* 2016, Chu *et al* 2021). Additional pieces of evidence include stochastic gradient boosting models that predict the existence of savannas in Asia using savanna climate envelopes from other continents (Ratnam *et al* 2016) and dynamic global vegetation models that simulated vegetation patterns using current climate (Kumar *et al* 2020, Scheiter *et al* 2020); the presence of high endemism and richness of $C_4$ grass species, which typify savannas (Ratnam *et al* 2016, Welker *et al* 2020, Chu *et al* 2021); and several *in situ* studies that have characterized the physiognomy, diversity, and fire-adapted traits of these communities in South and Southeast Asia (Khaing *et al* 2019, Nguyen *et al* 2019, Ratnam *et al* 2019).

Our research focuses on the parkland (PRK) and woodland (WDL) savannas of Yunnan Province in southwest China (figure 1), an elevated region with a strongly monsoonal and relatively dry climate (Shi *et al* 2017, Shi and Chen 2018) suitable for sustaining savannas and forests as alternative stable states (Bond *et al* 2005). In China, open-canopied PRK savannas were, until quite recently, only formally recognised in the dry valleys that incise Yunnan, and these have been subject to intense investigation (Jin and Ou 2000, Zhu *et al* 2020). The vegetation outside the dry valleys of Yunnan was previously classified as 'forest' with small patches of treeless grasslands recognised at higher elevations (Hou 2001). Their classification followed the Food and Agricultural Organization of the United Nations (FAO) definition of forests, in which vegetation with >10% tree cover is considered forest (Bastin *et al* 2017), but it is now well understood that the tree cover at which savanna switches to forest is between 60% and 80% (Hirota *et al* 2011, Staver *et al* 2011, Griffith *et al* 2017, Khaing *et al* 2019). A new vegetation map of China concluded that much larger swathes of Yunnan are comprised of vegetation with a grass-dominated ground layer (Su *et al* 2020). Northern Yunnan is presently dominated by pine and oak WDL savannas with denser canopies and a ground layer dominated by $C_4$ grasses, a vegetation widely distributed across higher elevation tropical Asia (Jin 2002, Ratnam *et al* 2016). Diversity in the valleys of Yunnan is well-researched with over 2000 plant species recorded (Jin 2002) among which there are at least 188 grass species, of which >80% are $C_4$ (Osborne *et al* 2014) dependent on open habitats, and 79 species belong to the Andropogoneae clade, which dominate fire-prone savannas worldwide (Ripley *et al* 2015). We are unaware of any published community studies of the savanna vegetation on the tablelands intervening the valleys. Nevertheless, there is strong evidence that $C_4$ savannas have been widely present in Yunnan since at least the early Pleistocene, placing their existence prior to any possible impact by hominins. The antiquity of the valley savannas is supported by fossil evidence indicating substantial $C_4$ presence and a switch from forest to grassy biomes at about 3.4–2 Ma (Biasatti *et al* 2012, Yao *et al* 2012). A phylogeographic study of two common $C_4$ Andropogoneae grasses in Yunnan has demonstrated that savannas have been present extensively across Yunnan in the valleys and across the intervening tablelands since the early Pleistocene, but possibly as early as the late Miocene (Chu *et al* 2021). At present, land conservation in Yunnan protects the Hengduan Mountains Biodiversity Hotspot in the northwest and different forest types found throughout the province (Zhao *et al* 2019a). Only one nature reserve has been specifically gazetted to protect the dry valley PRK savannas of Yuanjiang, and some montane grasslands are protected in the Hengduan Mountains and in limestone karsts in eastern Yunnan. The vast landscapes of WDL savannas are not viewed as conservation priorities, and as a result, their rates of loss under human impacts have not been evaluated.

Numerous assessments of landscape change using remotely sensed imagery have demonstrated rapid rates of human-driven vegetation loss in Yunnan (Xu *et al* 2007, Liu *et al* 2014b, Ning *et al* 2018, Zhang *et al* 2019a, 2019b), but these studies have not specifically assessed the spatiotemporal dynamics of PRK and WDL savanna coverage at the provincial scale. In addition, several national environmental policies have been put in place in China aiming for landscape protection, but with possible negative consequences for remaining intact savannas in Yunnan. Firstly, a national-level fire suppression policy has been effectively enforced since the late 1980s (Yi *et al* 2017), thereby limiting the occurrence of fires that are crucial for suppressing woody vegetation and maintaining savannas as open ecosystems in more humid environments (Bond 2019, Fogarty *et al* 2020). Second, a national-level ecological restoration project introduced during the 1990s called 'Grain To Green Program' (GTGP) halted the decrease of forests, which may have inadvertently led to significant afforestation of grassland areas in the southwest (Liu *et al* 2014b). In addition to direct land-use changes and landscape

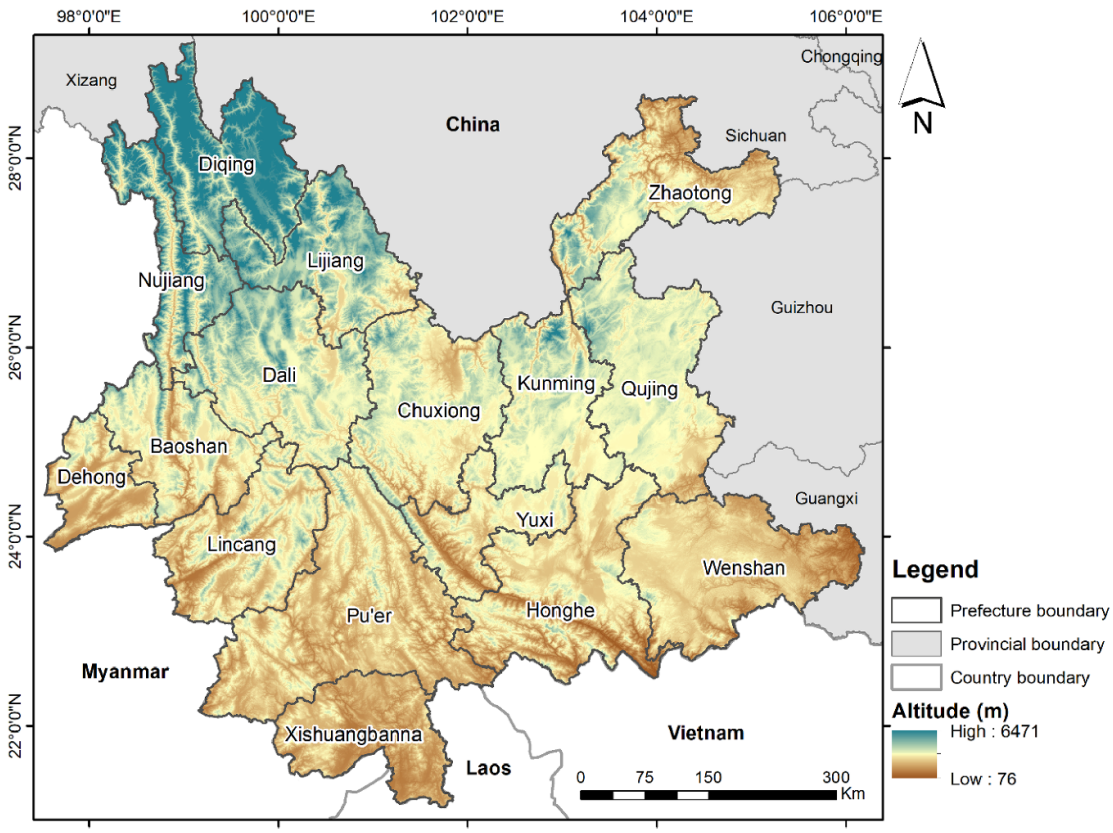


**Figure 1.** Map of Yunnan Province in southwest China with its autonomous prefectures. Colours indicate altitude; areas shaded brown are at lower elevation, while those shaded green are on higher elevation.

policies, increased atmospheric $CO_2$ may have been fertilizing the trees in Yunnan, in turn increasing their growth rates and causing increased woody encroachment (Buitenwerf *et al* 2012). Tree growth is suppressed by increased aridity and can be enhanced by increased temperature when water is not a limiting factor (Williams *et al* 2010, Panthi *et al* 2020), so it is probable that the changes in density in intact vegetation are happening faster in wetter and or warmer parts of Yunnan.

We analysed vegetation and land-use change in Yunnan for the period 1986–2016 (30 years of change) using Landsat imagery, which is the period over which the fire suppression policy and GTGP became effective (late 1980s and 1990s, respectively). Our specific objectives were to understand: (a) how much of the savanna vegetation had been lost and fragmented relative to the other major vegetation type in Yunnan, namely forest, (b) where savanna changes happened spatially across Yunnan and how much remained intact, and (c) which environmental drivers, either natural or anthropogenic, were associated to the changes in savanna across Yunnan.

## 2. Methods

To address the above objectives, we had five goals in our analysis: first was to assess the full extent of savanna physiognomy in Yunnan in 1986. Second was to quantify the rates of attrition and fragmentation of savannas versus forests in the province. Third, we sought to determine whether the savanna vegetation had undergone woody encroachment by explicitly defining two savanna vegetation classes that differ in woody plant canopy cover (PRKs and WDLs), and then measure the rates of change in these classes as well as forests (higher woody canopy cover). Fourth, we tested whether climate variables, fire, and landscape accessibility were correlated with changes in savanna canopy cover and transitions to other vegetation (forest) and land cover types. Fifth, aware of the low level of conservation of savannas in Yunnan, we identified savannas that have remained mostly intact over the last 3 decades as potential sites for future protected areas.

### 2.1. Generating land cover maps and detecting inter-decadal changes

Land cover maps of Yunnan were generated for years 1986, 1996, 2006, and 2016, encompassing 3 decades of change. Since we wanted to classify Landsat imagery as early as 1986, when no adequate reference data to train a supervised classifier was available, we used a hybrid of unsupervised and supervised techniques combined with knowledge-based interpretation (figure 2; see description of Yunnan and detailed methods in supplementary (available online at stacks.iop.org/ERL/17/014003/mmedia)).

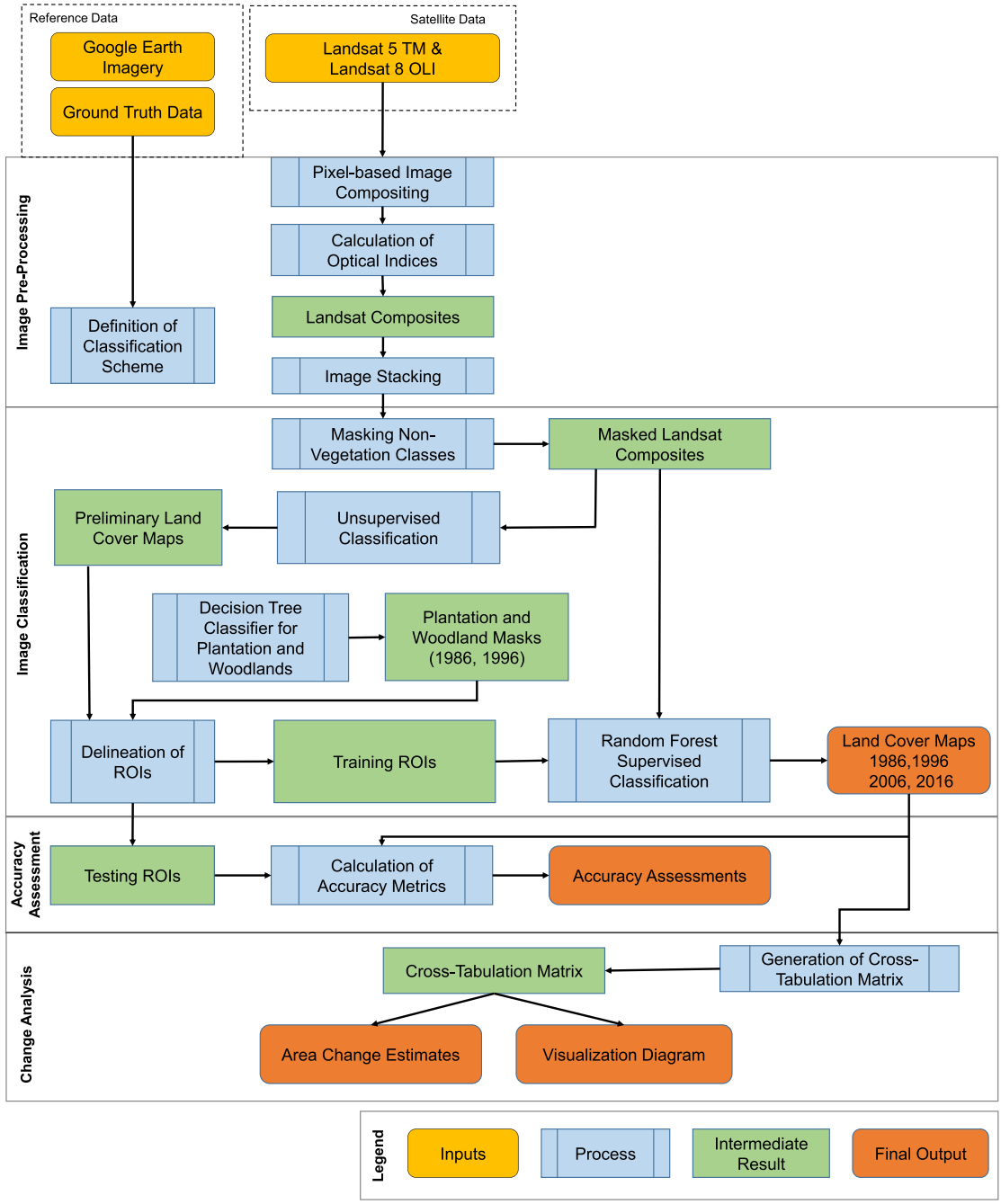


**Figure 2.** Overall workflow of the land cover classification and change analysis.

We first defined nine land cover classes in the province using a combination of field observations, expert knowledge coupled with visual inspection of high-resolution imagery from Google Earth (www.google.com/earth/desktop, accessed on 5 July 2019) (Olofsson *et al* 2014), and existing land cover maps (Liu *et al* 2003, 2010, 2014b, Xu *et al* 2005, Diallo *et al* 2009, Zhao *et al* 2012, Lu *et al* 2015, Ning *et al* 2018, Zhang *et al* 2019a, Su *et al* 2020). We defined nine land cover classes, comprised of non-vegetated classes, namely water bodies (WATs), snowed regions (SNO), and built-up and bare rock areas (BURs); non-natural vegetation areas, namely croplands (CROs), tree plantations (TRPs), and bare ground (BAG); and natural vegetation areas, which are forests (FOR), which have closed tree canopies, and two savanna classes, which have open canopies: grassy, sparse-canopied PRKs and denser-canopied WDLs. See supplementary tables 1 and 2 for their full descriptions.

Image composites used in the classification were generated for each mapping year from Google Earth Engine (GEE; http://earthengine.google.com) using a median ee.Reducer function that composited tier

1 calibrated top-of-atmosphere reflectance images obtained by Landsat-5 Thematic Mapper and the Landsat-8 Operational Land Imager available in the GEE image collection (Loveland and Dwyer 2012). The composites were comprised of seven spectral bands (BLUE, GREEN, RED, NIR, SWIR1, SWIR2, TIR) and were resampled from the original 30 m spatial resolution to 100 m using nearest neighbour method. Five spectral indices, which include normalized difference vegetation index (NDVI), enhanced vegetation index, soil-adjusted total vegetation index, normalized difference tillage index, and land surface water index, were also calculated for each study year and used to improve classifications (see supplementary S1.3). Each image stack per mapping year contained 12 image layers, consisting of the seven spectral bands and five indices.

To delimit the classification algorithms only to vegetation classes, we masked the non-vegetated classes (WAT, SNO, BUR) from the image stacks. These classes were separated using their NDVI (Running *et al* 1995) and thermal band (Price 1981) values determined using a decision tree algorithm (De Alban *et al* 2018; see supplementary S1.4.1). To aid in our delineation of regions-of-interest (ROI) polygons, we first ran unsupervised classification on the masked image stacks to generate a computer-automated classified image with 100 clusters in GRASS GIS (GRASS Development Team 2020). We then assigned each cluster to the remaining vegetated land cover classes (both natural and non-natural) through visual interpretation conducted by cross-checking the pixels of each cluster with true-colour (RED-GREEN-BLUE) and false-colour (NIR-RED-BLUE) image composites, as well as high-resolution imagery from Google Earth (available for 2006 and 2016) (Olofsson *et al* 2014).

The resulting maps from the unsupervised classification were then used to delineate ROIs for supervised classification. We performed stratified random sampling over the pixels from the unsupervised map to generate 500 points used as guides in drawing the ROIs. Each ROI (at least 1 $km^2$) was drawn around the points, with their extents delineated based on the potential homogeneity of the target land cover class. When delineating ROI polygons for 1986 and 1996, we utilised additional mask layers generated from 2016 image statistics to assist in locating TRP and WDL classes due to challenges in discerning them during visual interpretation of the older Landsat image composites and lack of high-resolution imagery for those years (see supplementary S1.4.4). ROIs were then divided for training (70%) and testing (30%).

For supervised classification, we used random forest (RF) (Gislason *et al* 2006, Rodriguez-Galiano *et al* 2012) (see supplementary S1.4.5 for RF parameterisation settings). We performed pixel-based accuracy assessment on the RF products by generating confusion matrices for each year, and computed the overall accuracy, user's and producer's accuracies, for each land cover class. We computed error-adjusted area estimations and the confidence intervals for each land cover class to quantify estimation uncertainties (Olofsson *et al* 2013). Vegetation maps from RF and the non-vegetation maps masked out earlier were combined, and isolated pixels were smoothed out using a Majority Filter tool to produce final maps. The raster operations, supervised classification, and accuracy assessments were performed in R (R Core Team 2021), while smoothing was performed in ArcMap (ESRI 2011).

To detect inter-decadal land cover change dynamics, we utilised the final maps to produce cross-tabulation matrices that summarised the land cover changes from 1986 to 2016 using the Semi-Automatic Classification Plugin in Quantum GIS (Congedo 2014). We used the older map as the 'reference map' and more recent map as the 'classification map' (i.e. to detect change between 2006 and 2016, we used the 2006 map as 'reference' and the 2016 map as 'classification'). To visualize the land cover changes, we created Sankey diagrams using the networkD3 package (Allaire *et al* 2017) in R.

### 2.2. Assessing the fragmentation and legal protection levels of savannas and forests

We calculated fragmentation statistics for natural vegetation classes PRK savanna, WDL savanna, and forest (FOR) for each mapping year. These included number of fragments, size of fragments (mean patch area, largest patch index), geometric complexity (mean patch shape ratio), physical connectedness (patch cohesion index), and edge density. These were calculated using the landscapemetrics package in R (Hesselbarth *et al* 2019).

We also determined the level of protection that each land cover types received in 2016 by calculating their areal extents within Yunnan protected areas provided by CAS-RESDC (www.resdc.cn/data.aspx?DATAID=272, accessed on 16 May 2021). We also located persistent savanna areas by identifying unchanged pixels of PRK and WDL since 1986, and subsequently derived the number of decades a pixel had remained as PRK or WDL.

### 2.3. Determining drivers of change in savanna coverage

We conducted logistic regression analyses to assess whether retention or conversion of savannas to other land cover types were due to selected environmental

parameters, including climate (mean annual temperature (MAT), aridity), topography (slope), presence of fire (hereafter referred to only as 'fire'), and accessibility (distance from the nearest road (hereon referred to only as 'distance')). MAT and aridity both impact plant growth rates (Williams *et al* 2010, Panthi *et al* 2020), and hence rates of vegetation change. Fire reduces tree biomass, which helps to maintain open ecosystems such as savannas (Higgins *et al* 2000, Lehmann *et al* 2009). Slope and distance both constrain human accessibility and thus direct human impacts (Liu *et al* 2014a, Alphan 2017).

To assess drivers of woody encroachment, we analysed transitions of savanna to denser vegetation (PRK to WDL, PRK to FOR, and WDL to FOR). To assess drivers of fragmentation from land use conversion, we investigated transitions of PRK and WDL to/from farmlands and non-vegetation classes. In these analyses, we lumped together CRO, TRP, and BAG under one 'farmland' class, and BUR, WAT, and SNO under one 'non-vegetation' class. To quantify land cover change, we reclassified the transition maps into binary according to the transition being analysed. Pixels that retained their classification in the next time step were scored '0', while those that transitioned to another were scored '1'.

As we were interested in state changes between two levels (i.e. 0 and 1) in each analysis, we tested predictors of land cover transitions using logistic regression in R. Environmental data of both '0' and '1' pixels were first extracted using the extract() function of the raster package in R. The pixels environmental data served as predictors, while their land cover transition scores represented the change variable in the regression models. We used MAT, aridity, slope, and fire in analysing PRK and/or WDL conversion to denser-canopied WDL and FOR to test whether these predictors were responsible for inducing or preventing canopy closure. We added distance in assessing PRK and WDL conversion to/from farmland to investigate whether accessibility influenced land cover change. In testing PRK and WDL conversion to/from non-vegetation, we used slope, distance, and fire. We transformed predictors as needed to approximate normality prior to regression. To assess the robustness of predictor coefficients, we ran the model for each type of transition 1000 times using randomly subsampled equal populations of 1's and 0's for each run, and constructed 95% quantile intervals for each coefficient; 95% quantile intervals which did not overlap zero were considered significant. The explanatory power for each significant predictor was computed from the median of all the partial *R*-squared values calculated using the partR2 package (Stoffel *et al* 2021) across all runs. We analysed changes across 3 decades (1986–2016) and decadal changes (1986–1996; 1996–2006; 2006–2016). Analyses were conducted at 1 km resolution to match the native resolution of available environmental data. Sources of environmental data are listed in supplementary S2.

## 3. Results

### 3.1. Accuracy assessment

Accuracy for the supervised classification of vegetation land cover types were 77.89% ± 1.31%, 82.16% ± 1.19%, 94.93% ± 0.69%, and 86.84% ± 1.06% for the 1986, 1996, 2006, and 2016 maps, respectively (see supplementary table S3). For PRK savannas, user's accuracy values (UA) ranged from 81.4% to 96.8%, while producer's accuracy values (PA) were 72.8%–92.3%, with the lowest and highest values from 1986 to 2006, respectively. For WDL savannas, UA ranged from 69.7% to 91.8% and PA ranged from 75.2% to 95.8%. Most of the misclassified PRK pixels belonged to CRO, BAG, and WDLs, while most of the misclassified WDLs were in PRKs and FORs, particularly during 1986 and 1996 (see supplementary table S4 for error matrices). Forest had high values for both UA (93.3%–99.2%) and PA (85.5%–97.3%).

### 3.2. Net changes over 3 decades, 1986–2016

In 1986, the majority of Yunnan was covered by natural vegetation (figure 3). The combined savanna classes covered 40.30% of the landscape, with PRK savannas at 27.09% and WDL savannas at 13.21%, while FOR was at 30.78%. There were also substantial CROs at 17.73%, while TRPs had low cover at 3.33%. BAG covered 5.38%, whereas BUR was at 1.72%. WATs and SNO regions had the lowest coverage at 0.48% and 0.28%, respectively.

By 1996, savannas had a net increase of 2.26%, as PRK cover increased by 4.29% and WDL declined by 2.03%. FOR cover increased by 1.69%. CROs dropped by 4.85%, but BAG increased 1.67%. In 2006, savannas declined slightly due to a 6.32% drop in PRK areas despite a 5.35% increase in WDLs. Decreases in FOR (0.92%), CRO (0.74%), and BAG (1.47%) coverage occurred while TRPs (3.91%) and BURs (0.27%) increased.

By 2016, PRK savanna coverage substantially declined 8.56%, while WDL savanna slightly decreased 0.78%, bringing the overall savanna decline to 9.34%. Forest cover only had a slight decrease of 0.16%, whereas CRO (2.11%) and plantation (1.48%) coverage increased. The highest increases in BAG (4.15%) and BUR (1.30%) were observed this decade.

### 3.3. Losses and gains in savanna coverage

Extensive land cover changes were observed in Yunnan between 1986 and 2016 (figure 4; see supplementary S5 for the land cover change matrices), and a total of 316 800 km$^2$ (74.7% of Yunnan's total land area) underwent change. The gross gains and losses

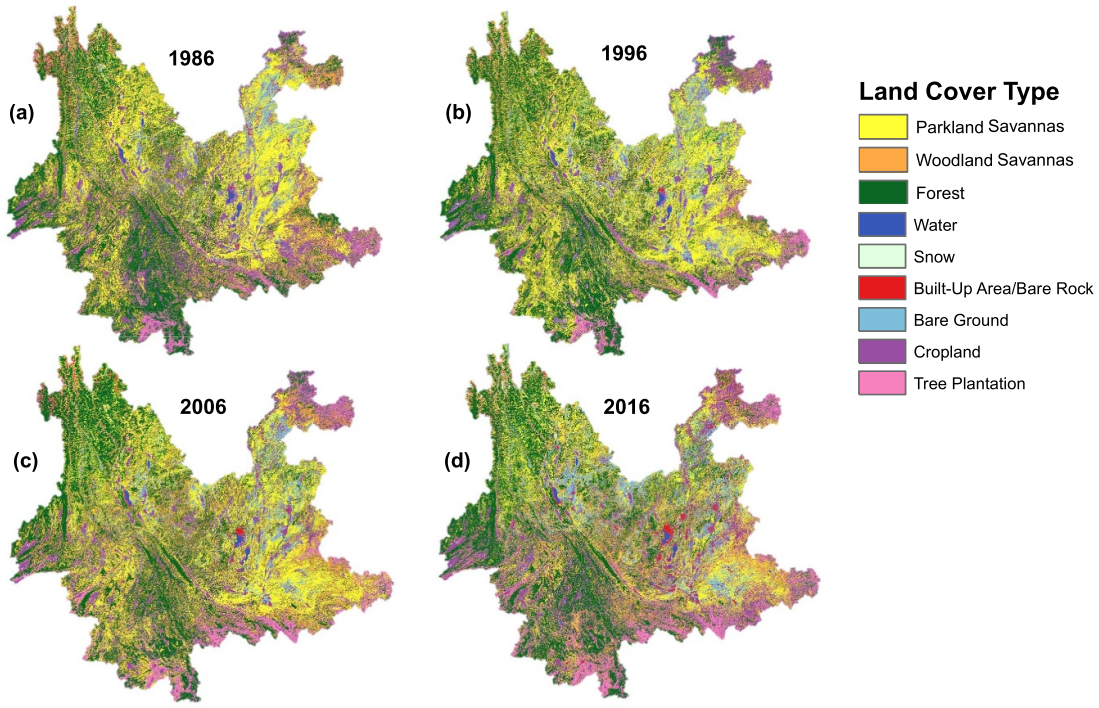


**Figure 3.** Land cover maps of Yunnan Province, China for (a) 1986, (b) 1996, (c), 2006, and (d) 2016.

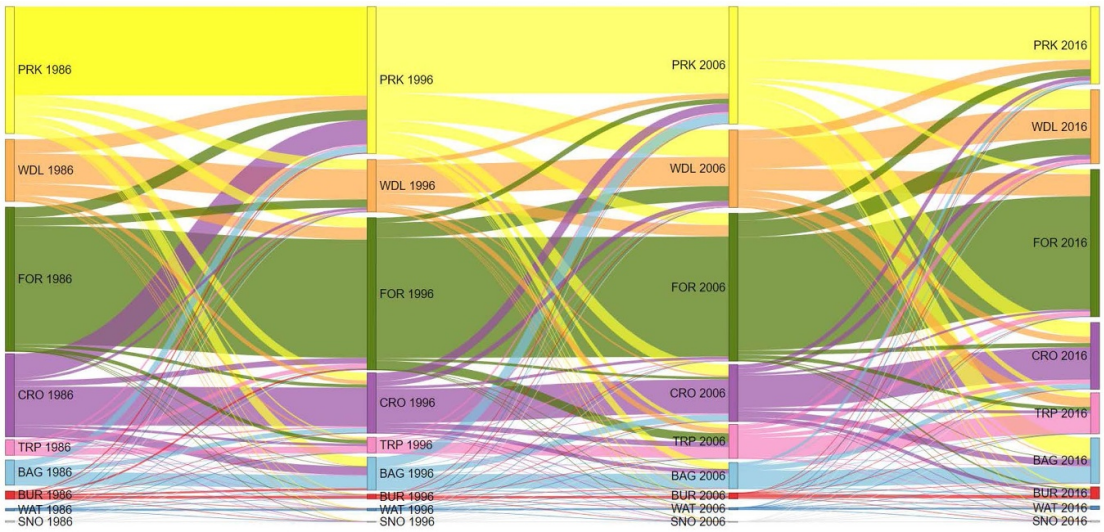


**Figure 4.** Sankey diagram of the land cover transitions in Yunnan Province, China from 1986 to 2016. Nodes indicate the land cover percentage for each particular time step, while the ribbons depict the transitions between land cover types. Colours follow that of the land cover map (figure 3). Note: PRK: parkland, WDL: woodland, FOR: forest, CRO: cropland, TRP: tree plantations, BAG: bare ground, BUR: built-up area and bare rock, WAT: water bodies, SNO: snow.

within each land cover type indicated dynamic transitions throughout the study period. The observed decline in PRK savanna cover was largely due to woody cover increases to WDL savanna (5.60%) and FOR (3.66%), and direct land conversion to CRO (2.88%), BAG (4.04%), plantations (0.98%) and BUR (0.31%). Most PRK savanna that was persistent until 2016 was on the eastern and northwest sections of Yunnan (figures 5(a) and 6). Gains in PRK savanna were scattered across the upper section of province, with a concentration of converted WDL savanna and CRO to PRK savanna in the east (figure 5(b)).

Total WDL savanna coverage was very dynamic. Persistent WDL savanna was ∼6% of 13.21% in 1986, but the remainder changed substantially mostly due to tree cover changes between PRK savanna and FOR

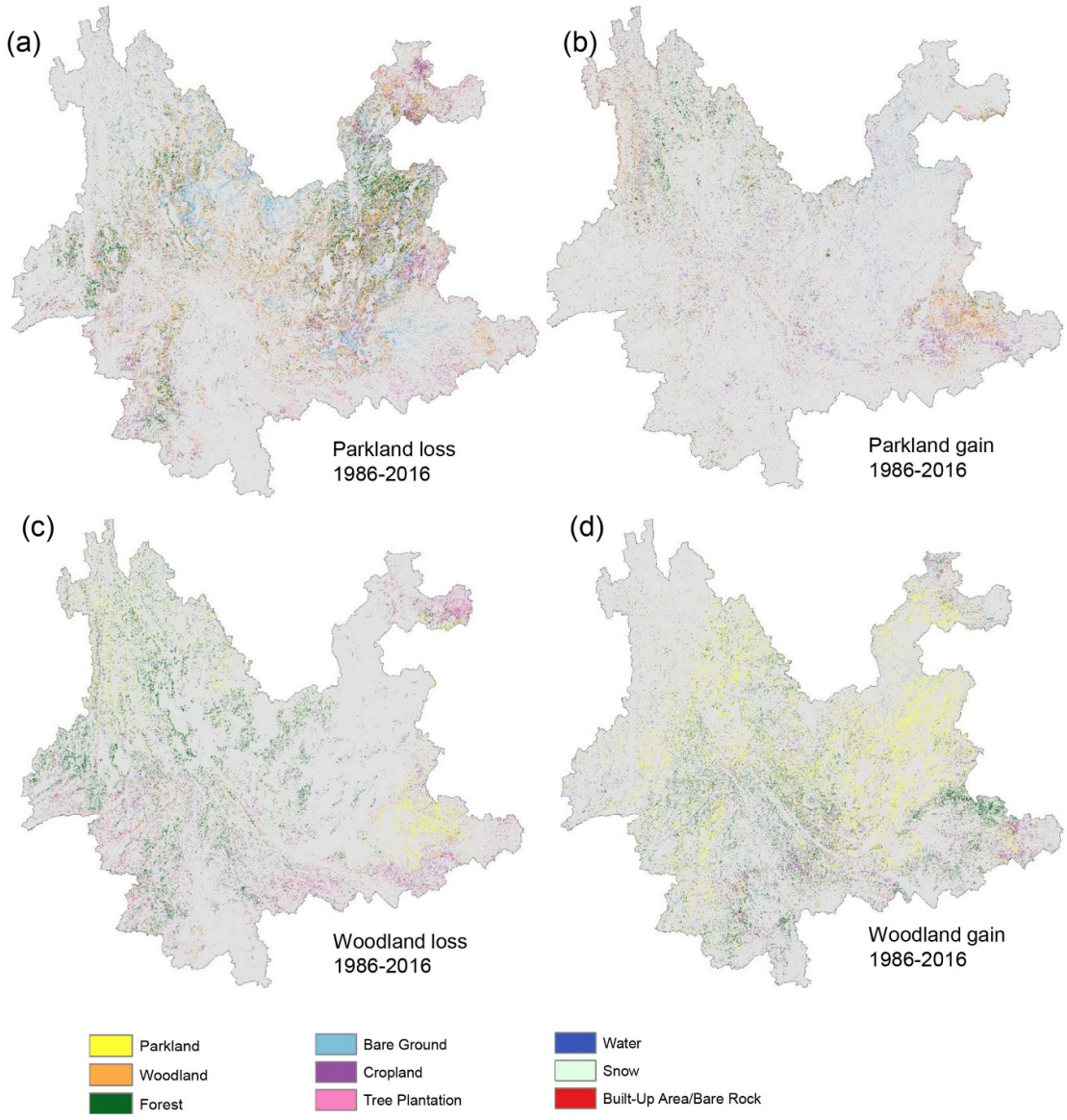


**Figure 5.** PRK (a), (b) and WDL (c), (d) loss and gain between 1986 and 2016 in Yunnan Province, China. Colours in 'loss' figures (a), (c) depict land cover classes which PRK and WDL transitioned to, while colours in 'gain' figures (b), (d) represent classes from which PRK and WDL gained coverage from.

states, and also through conversion to TRPs in the south and northeast (figure 5(c) and (d)).

### 3.4. Fragmentation and protected area coverage analyses of natural vegetation cover types

Fragmentation generally increased for all natural vegetation land cover types from 1986 to 2016, but was more severe for savannas (table 1). The number of patches increased during this period for PRK savannas (29.3%), WDL savannas (59.8%), and FOR (23.9%). Fragment sizes also generally decreased, most severely for PRK, with mean patch area decreasing 52.9% (from 20.25 ha to 9.53 ha) between 1986 and 2016. The mean patch areas of WDL (25.3%) and FOR (17.8%) decreased less. The largest patch index for PRK also decreased dramatically, from 6.84 to 0.33 between 1986 and 2016. In contrast, the largest patch index values of WDL (0.17 vs 0.15) and FOR (2.78 vs 2.97) had changed less during the same period. The edge density of WDLs (21.30 vs 29.77) and FORs (24.08 vs 25.57) increased, but decreased for PRKs (27.16 vs 25.56). Fragment connectivity of savannas decreased, with PRK (99.65%–96.23%) experiencing greater loss than WDL (93.28%–91.87%), whereas it remained stable for FOR (99.52%–99.43%). The geometric complexity of the fragments, as indicated by the mean patch shape ratio, was largely stable across time for savannas and forests.

The protected area coverage analysis indicated low legal protection percentages for all natural vegetation land cover types for 2016. Of the three, FOR had the most legal protection, with 7.60% (10 127 $km^2$ out of 133 160 $km^2$ total 2016 coverage) inside protected area boundaries. The savannas had lower protection, with PRK at 3.09% (2161/70 022 $km^2$), and WDL at 1.84% (1233/66 824 $km^2$). In addition,

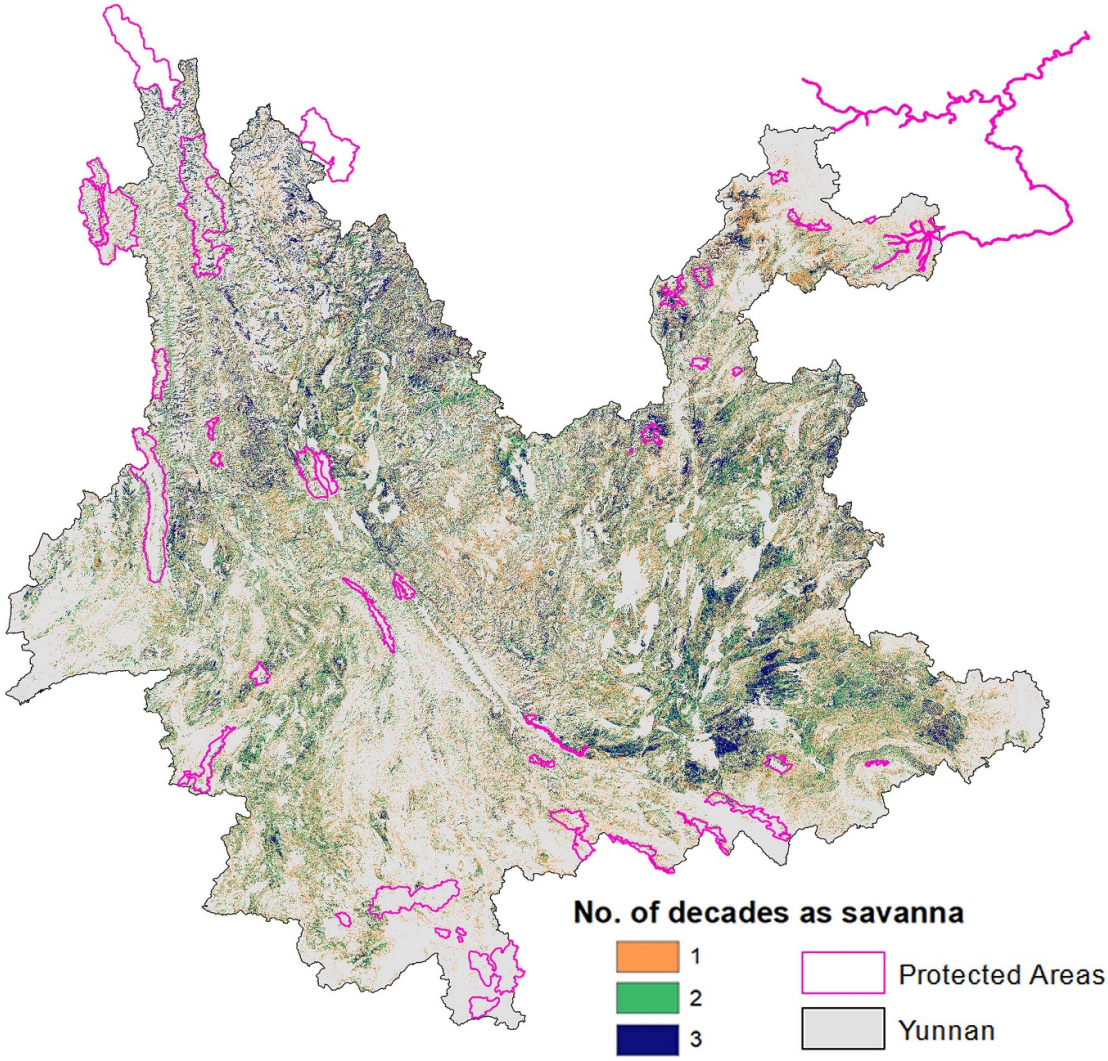


**Figure 6.** Map of Yunnan Province, China showing savannas (PRKs and WDLs) with existing protected area boundaries (outlined in pink) from the Resource and Environment Science and Data Center of the Chinese Academy of Sciences. Colours indicate the age of savannas, with dark blue depicting savannas with 3 decades (1986–2016) of stability.

most of these nature reserves do not cover the persistent savanna fragments (figure 6). PRK protection is only 11.96% (2161 km$^2$ out of 18 064 km$^2$ total nature reserve area), while WDL is at 6.82% (1233/18 064 km$^2$). In contrast, FOR protection is at 56.06% (10 127/18 064 km$^2$), a clear indication that savannas are underrepresented in most of the protected areas.

### 3.5. Drivers of change in savannas

The logistic regression models indicated varying significant associations between the different environmental parameters and land cover changes between and across the 3 decades (table 2). In the PRK savanna to WDL savanna and FOR transitions, the general trend in between decades indicated that PRK savannas located in warmer and wetter (more positive aridity index) areas had a greater probability to transition to denser-canopied vegetation (WDL savanna or FOR). Although the overall analysis suggested that PRK in drier areas transitioned to WDL, aridity only weakly explained the variation (lowest partial $R^2$) in this case. For WDL savanna to FOR transitions, WDL in wetter regions converted to FOR. The effect of temperature differed in between decades; however, the overall transition suggested that WDL in colder areas became FOR. While the effect of slope varied per decade, the overall analyses suggested that PRK in gentler slopes (negative trend) converted to WDL, and WDL in steeper slopes (positive trend) converted to FOR. Fire had a negative effect on transitions to denser canopy cover. In the majority of these transitions, MAT was the predictor explaining the most variation.

Fire was positively related to conversion of WDL and FOR to more open PRK and WDL, but the rest of the predictors had variable effects in these transitions. The analyses suggested that WDLs in colder, wetter, and steeper regions converted to PRKs, and that FORs in drier and flatter places switched to PRK and WDL. MAT had a generally positive trend across the decades, suggesting that transitions to more open vegetation happened in warmer areas. Overall, FOR to PRK

**Table 1.** Fragmentation statistics of PRK savanna, WDL savanna, and FOR cover types for each year.

| Land cover type | Year | Number of patches | Mean patch area (ha) | Largest patch index (%) | Mean patch shape ratio | Edge density (m ha$^{-1}$) | Patch cohesion index (%) |
|---|---|---|---|---|---|---|---|
| PRK savanna | 1986 | 510 234 | 20.25 | 6.84 | 1.29 | 27.16 | 99.65 |
| | 1996 | 411 436 | 29.18 | 9.91 | 1.33 | 30.27 | 99.78 |
| | 2006 | 438 202 | 21.87 | 3.66 | 1.32 | 26.68 | 99.36 |
| | 2016 | 659 646 | 9.53 | 0.33 | 1.28 | 25.56 | 96.23 |
| WDL savanna | 1986 | 476 306 | 10.62 | 0.17 | 1.34 | 21.30 | 93.28 |
| | 1996 | 479 747 | 8.90 | 0.02 | 1.32 | 19.04 | 89.40 |
| | 2006 | 494 792 | 12.80 | 0.26 | 1.34 | 24.50 | 95.89 |
| | 2016 | 761 255 | 7.93 | 0.15 | 1.33 | 29.77 | 91.87 |
| FOR | 1986 | 331 344 | 35.60 | 2.78 | 1.33 | 24.08 | 99.52 |
| | 1996 | 303 699 | 40.93 | 4.52 | 1.34 | 23.57 | 99.54 |
| | 2006 | 360 306 | 33.48 | 3.08 | 1.32 | 23.75 | 99.39 |
| | 2016 | 410 501 | 29.26 | 2.97 | 1.29 | 25.57 | 99.43 |

transitions happened in colder places, while FOR to WDL occurred in warmer spots. MAT and aridity were the most important predictors in explaining variation.

PRK and WDL that converted to farmlands during 1986–2016 were generally in warmer, wetter areas close to road networks and had no fire occurrence. PRK that converted to farms were in flatter places, while WDL that did were in steeper slopes. On the reverse side, farmlands that became PRK or WDL were in colder, steeper regions far from roads and had experienced fire. Moreover, there is a clear trend of wetter farmlands becoming WDL, while the trend for PRK is unclear. In these transitions, MAT, aridity, distance, and slope explained most of the variation in the data.

PRK conversion to non-vegetation areas were also in gentler slopes and near roads. Transitions to non-vegetation classes from 1986 to 2006 happened in colder PRKs. However, the overall transition suggested that PRK in warmer and wetter areas converted to non-vegetation. The overall WDL to non-vegetation transition had similar results, although there were insufficient data to analyse inter-decadal transitions for 1986–2006 due to the small percentage of WDL areas that were converted to non-vegetation areas. Conversely, non-vegetation areas that became PRK and WDL were located in steeper areas and far from roads. In addition, non-vegetation areas in warmer areas became WDL overall. Distance and slope explained most of the variation, whereas fire yielded non-significant associations.

## 4. Discussion

### 4.1. Accuracy

While the overall accuracy numbers we obtained were acceptable for our analyses and comparable to other large-scale land cover studies (Bruggeman *et al* 2016, Su *et al* 2020), we observed variations among decades. We attribute these to the different locations of the training ROIs used for each time step, despite ensuring the stability of their spectral signatures (see boxplots in supplementary S1.4.3). It was easier to discern between classes for 2006 and 2016, with high-resolution imagery available to guide ROI sampling, but more challenging for 1986 and 1996. Nevertheless, the UA and PA numbers we obtained for PRK and WDL savannas were well within reasonable range, and thus reliable for analysing trends in savanna cover. Focusing on UA/PA of target land cover classes, which were savannas in our case, is included in the 'good practice' recommendations for area change and accuracy assessment (Olofsson *et al* 2014). The confidence intervals from the area-adjusted accuracy computations indicate that misclassified areas only comprise a small percentage of the total area of the savanna classes. These misclassified areas were between PRKs and CRO/BAG (see confusion matrices in supplementary S4), which could be due to similarity in spectral signatures of these classes, as grasses are the main vegetation in both classes. During field observations, we noticed some farmlands occur interspersed in between PRKs, which may have contributed to the confusion given the 100 m resolution used in the study. A finer-scale classification, however, would be less useful as our aim is to depict trends in savanna dynamics of a large area (~400 000 km$^2$); the environmental data are also only available in coarser resolution, thus, the land cover data would always be aggregated to accommodate the drivers of change analyses. We improved the separation of these classes by including spectral indices in the classification.

### 4.2. Dynamic land cover changes in Yunnan exposed the loss of savanna coverage

Our spatial analyses showed that savannas were much more extensive in Yunnan than previously mapped, accounting for 40.3% of Yunnan's land area in 1986, and that savannas were not only limited to the hot

**Table 2.** ANOVA results for generalized linear regression analyses testing whether conversion of land cover types are driven by MAT, aridity, slope, presence of fire, or distance from roads. To achieve a normal distribution required by the model, aridity and slope were transformed using square root, while distance from roads was log10-transformed. For each land cover transition, columns under the time periods list each significant ($P < 0.001$) predictor's coefficient sign and partial $R^2$, while ns means not significant, and nd means no data, thus not included in the analysis.

| | | Overall | | 1986–1996 | | 1996–2006 | | 2006–2016 | |
|---|---|---|---|---|---|---|---|---|---|
| | Variable | Trend | Partial $R^2$ | Trend | Partial $R^2$ | Trend | Partial $R^2$ | Trend | Partial $R^2$ |
| PRK to WDL | MAT | + | 0.0359 | − | 0.0095 | + | 0.0084 | + | 0.0536 |
| | Aridity | − | 0.0008 | + | 0.0027 | + | 0.0023 | ns | |
| | Slope | − | 0.0023 | + | 0.0295 | + | 0.0006 | — | 0.0009 |
| | Fire | − | 0.0020 | nd | | ns | 0.0003 | — | 0.0015 |
| | *n* | 63 722 | | 88 722 | | 102 396 | | 65 082 | |
| PRK to FOR | MAT | + | 0.0035 | − | 0.0286 | + | 0.0025 | + | 0.0126 |
| | Aridity | + | 0.0045 | + | 0.0044 | − | 0.0010 | + | 0.0023 |
| | Slope | ns | 0.0003 | + | 0.0090 | ns | | ns | |
| | Fire | − | 0.0082 | nd | | − | 0.0012 | − | 0.0058 |
| | *n* | 55 896 | | 88 772 | | 88 665 | | 51 962 | |
| WDL to FOR | MAT | − | 0.0055 | + | 0.0011 | − | 0.1748 | ns | |
| | Aridity | + | 0.0073 | + | 0.0020 | + | 0.0128 | + | 0.0118 |
| | Slope | + | 0.0046 | − | 0.0034 | ns | | + | 0.0044 |
| | Fire | − | 0.0068 | nd | | − | 0.0004 | − | 0.0055 |
| | *n* | 31 510 | | 37 860 | | 36 115 | | 45 986 | |
| WDL to PRK | MAT | − | 0.0179 | + | 0.0375 | − | 0.0351 | − | 0.0273 |
| | Aridity | + | 0.0105 | + | 0.0066 | + | 0.0018 | − | 0.0016 |
| | Slope | + | 0.0005 | − | 0.0373 | + | 0.0042 | + | 0.0058 |
| | Fire | + | 0.0076 | nd | | + | 0.0050 | + | 0.0049 |
| | *n* | 22 943 | | 39 656 | | 30 775 | | 34 521 | |
| FOR to PRK | MAT | − | 0.0218 | + | 0.0522 | + | 0.0046 | − | 0.0848 |
| | Aridity | − | 0.0618 | − | 0.0471 | − | 0.0420 | − | 0.0549 |
| | Slope | − | 0.0023 | − | 0.0158 | − | 0.0033 | ns | |
| | Fire | + | 0.0161 | nd | | + | 0.0132 | + | 0.0143 |
| | *n* | 96 676 | | 115 556 | | 112 905 | | 108 601 | |
| FOR to WDL | MAT | + | 0.0569 | − | 0.0062 | + | 0.0349 | + | 0.0283 |
| | Aridity | − | 0.0255 | ns | | − | 0.0016 | − | 0.0366 |
| | Slope | − | 0.0071 | − | 0.0118 | − | 0.0123 | − | 0.0052 |
| | Fire | + | 0.0044 | nd | | + | 0.0007 | + | 0.0033 |
| | *n* | 106 291 | | 113 234 | | 121 767 | | 117 058 | |
| PRK to farmland | MAT | + | 0.0808 | + | 0.0160 | + | 0.0451 | + | 0.0997 |
| | Aridity | ns | | + | 0.0042 | ns | | − | 0.0013 |
| | Slope | − | 0.0053 | − | 0.0022 | − | 0.0012 | − | 0.0027 |
| | Fire | − | 0.0015 | nd | | − | 0.0007 | − | 0.0011 |
| | Distance | − | 0.0085 | − | 0.0132 | − | 0.0100 | − | 0.0052 |
| | *n* | 73 249 | | 96 005 | | 97 053 | | 82 671 | |
| WDL to farmland | MAT | + | 0.1322 | + | 0.1235 | + | 0.1393 | + | 0.0645 |
| | Aridity | + | 0.0546 | + | 0.0382 | + | 0.0276 | + | 0.0495 |
| | Slope | + | 0.0092 | − | 0.0202 | ns | | + | 0.0118 |
| | Fire | − | 0.0022 | nd | | − | 0.0014 | − | 0.0015 |
| | Distance | − | 0.0039 | − | 0.0294 | − | 0.0051 | − | 0.0011 |
| | *n* | 29 327 | | 31 996 | | 32 079 | | 41 176 | |
| Farmland to PRK | MAT | − | 0.0857 | − | 0.0257 | − | 0.0179 | − | 0.0698 |
| | Aridity | ns | 0.0003 | + | 0.0013 | ns | | − | 0.0025 |
| | Slope | + | 0.0143 | + | 0.0151 | + | 0.0068 | + | 0.0094 |
| | Fire | + | 0.0030 | nd | | + | 0.0012 | + | 0.0032 |
| | Distance | + | 0.0120 | + | 0.0317 | + | 0.0108 | + | 0.0049 |
| | *n* | 59 914 | | 81 375 | | 71 212 | | 67 998 | |
| Farmland to WDL | MAT | − | 0.0081 | − | 0.0081 | − | 0.0321 | Ns | |
| | Aridity | + | 0.0075 | + | 0.0588 | + | 0.0509 | + | 0.0060 |
| | Slope | + | 0.0189 | + | 0.0649 | + | 0.0282 | + | 0.0181 |
| | Fire | + | 0.0006 | nd | | ns | | ns | |
| | Distance | + | 0.0202 | + | 0.0394 | + | 0.0349 | + | 0.0126 |
| | *n* | 59 253 | | 55 857 | | 58 924 | | 69 492 | |

(Continued.)

**Table 2.** (Continued.)

| | | Overall | | 1986–1996 | | 1996–2006 | | 2006–2016 | |
|---|---|---|---|---|---|---|---|---|---|
| | Variable | Trend | Partial $R^2$ | Trend | Partial $R^2$ | Trend | Partial $R^2$ | Trend | Partial $R^2$ |
| PRK to non-vegetation | MAT | + | 0.0036 | − | 0.1046 | − | 0.1467 | ns | |
| | Aridity | + | 0.0087 | ns | | ns | | ns | |
| | Slope | − | 0.0164 | − | 0.0495 | − | 0.0094 | − | 0.0066 |
| | Fire | ns | | nd | | ns | | − | 0.0028 |
| | Distance | − | 0.0594 | − | 0.0296 | − | 0.0577 | − | 0.0196 |
| | *n* | 41 757 | | 80 173 | | 78 465 | | 49 458 | |
| WDL to non-vegetation | MAT | + | 0.0237 | | | | | ns | |
| | Aridity | + | 0.0520 | | | | | − | 0.0552 |
| | Slope | − | 0.0126 | nd | | nd | | ns | |
| | Fire | ns | | nd | | nd | | ns | |
| | Distance | − | 0.0359 | nd | | nd | | + | 0.0114 |
| | *n* | 14 386 | | | | | | 26 318 | |
| Non-vegetation to PRK | MAT | ns | | − | 0.0039 | ns | | ns | |
| | Aridity | ns | | ns | | ns | | ns | |
| | Slope | + | 0.0502 | + | 0.0396 | + | 0.0337 | + | 0.1534 |
| | Fire | ns | | nd | | ns | | ns | |
| | Distance | + | 0.0039 | ns | | ns | | + | 0.0258 |
| | *n* | 5249 | | 5565 | | 4582 | | 5393 | |
| Non-vegetation to WDL | MAT | + | 0.0518 | − | 0.0677 | | | | |
| | Aridity | ns | | ns | | | | | |
| | Slope | + | 0.0907 | ns | | nd | | nd | |
| | Fire | ns | | nd | | nd | | nd | |
| | Distance | ns | | ns | | nd | | nd | |
| | *n* | 4565 | | 4697 | | | | | |

dry valleys of the province. This is direct land cover evidence that savannas indeed exist in Yunnan, as postulated by spatial models derived from climate spaces of savannas from other continents (Ratnam *et al* 2016) and by larger scale dynamic global vegetation model simulations of tropical east Asian vegetation (Scheiter *et al* 2020). The more detailed canopy-based classification scheme we used divided the previously mapped 'forests' based on the FAO definition, and thus gave more resolution to the vegetation types existing in Yunnan. PRKs occupied almost the entire northern and eastern regions of the province, then extended westward to Kunming Prefecture and the Dali-Lijiang area in the northwest, and southward to Lincang. WDLs were extensive in the northeast along the border with Guizhou province, in the Wenshan area on the southeast, and occurred as transitions between PRKs and FORs in other parts of Yunnan.

Savannas declined by 8% in coverage over the 30 years due to the overall decrease in PRK areas, despite a small increase of WDLs. We observed two notable losses in PRK cover. First was the massive loss of PRKs converted to BAGs and CROs, which occurred concurrently with conversions of cropland to urban areas and plantations. This is corroborated by local-scale studies in the Hengduan mountains during 1990–2010 (Wang *et al* 2018) and 2000–2012 (Wu *et al* 2015), and in the Dianchi Lake watershed where a 62.1% decline in grassland cover during 1974–2008 was observed (Zhao *et al* 2012), mostly through conversion to urban and agricultural land. These PRK to farmland conversions occurred in warmer, gently sloped areas accessible via road networks, whereas PRK to built-up area conversions took place in plateaued areas near roads. The most significant drivers explaining these transitions were in areas with relatively warmer temperature and closer proximity from roads.

Second, substantial areas of PRK converted to WDL and then to FOR, indicating woody plant encroachment across Yunnan Province. These transitions occurred throughout the study period, but most were apparent during 2006–2016, and in more humid environments that experienced no fire. This was observed in a local-scale land cover assessment of Greater Kunming, where 1200 km$^2$ of grassland were converted to forest and thickets from 2003 to 2010 (Lu *et al* 2015). These transitions may possibly be due to afforestation, fire suppression, atmospheric $CO_2$ enrichment, or a combination of all. In our analysis, PRKs in steeper regions converted to WDLs during 1996–2006, coinciding with previous observations that open grasslands converted to woodlands in montane areas of southwest China due to implementation of the GTGP during this period (Liu *et al* 2014b). Fire was negatively associated with transitions to denser canopy cover vegetation and positively associated with transitions to more open vegetation, suggesting fire could promote the persistence of open PRKs in Yunnan, as in other ecosystems (Fogarty *et al* 2020). Atmospheric $CO_2$

enrichment increases the growth efficiency of $C_3$ trees (Ehleringer *et al* 1997, Hoffmann *et al* 2000, Kgope *et al* 2010), and is suggested to be responsible for woody encroachment in savannas in Africa (Buitenwerf *et al* 2011). Model simulations of tropical and subtropical Asian vegetation have also suggested that elevated $CO_2$ is supporting woody plant biomass increases and vegetation transitions (Scheiter *et al* 2020).

### 4.3. Fragmentation of savannas in Yunnan is greater than for other vegetation types

Although all three natural vegetation types experienced greater fragmentation over time, PRKs suffered the worst degradation, breaking into smaller patches with greater exposed edges and less connectivity. WDLs suffered a massive increase in patch number during 2006–2016, after being relatively stable from 1986 to 2006; however, their connectivity slightly increased throughout the decades. Fragment numbers also increased in FORs, but the largest forest fragments increased and patch cohesion barely changed throughout the decades. The decrease in connectivity of savanna fragments can negatively affect grassland species, which respond sensitively to fragmentation introduced by woody species (Fuhlendorf *et al* 2002, Cunningham and Johnson 2019), and can introduce disruptions in genetic flow between populations (Honnay *et al* 2007, Helm *et al* 2009), affecting the biodiversity supported by these habitats (Jin 2002, Simon *et al* 2009, Ratnam *et al* 2016). To our knowledge, these are the first fragmentation statistics of Yunnan's savannas. Existing fragmentation research in the region only focused on forests (Liang *et al* 2014, Liu *et al* 2017, 2020, Zhang *et al* 2019a, Zhao *et al* 2019b). Our results suggest that fragmentation of savannas is severe and requires urgent attention.

### 4.4. Conservation recommendations

Our analysis suggests that Yunnan's forest cover was largely stable, and even experienced a slight increase over the 3 decades. Forests also possessed a higher level of protection among the two vegetation types. These, combined with the fact that forest fragmentation was also less compared to savannas, imply that the implementation of the GTGP and the protected area systems in place are effectively protecting forests, despite the low protection coverage relative to the total forest land area. The province might also continue to observe an uptick in stable forest cover, as China continues its existing programs to conserve and expand forests (Chen *et al* 2019). Policies affecting Yunnan include the sloping land conversion program (SLCP) to prevent cultivation on land with slopes steeper than 25° (Xu *et al* 2005), and the GTGP established in 1999 to restore natural ecosystems through the return of former croplands back to forests or savannas (Chen *et al* 2019). A good policy model for savannas could be the SLCP, as our drivers analysis showed that steeper slopes did in fact contribute positively to PRK and WDL conversion from farmlands and non-vegetation areas. Well-informed implementation of the GTGP on former farmlands rather than PRKs would also be helpful. A policy regarding the controlled use of fire would also be beneficial for savanna protection, as its presence was demonstrated to be favourable for retaining savannas. The use of fire for maintaining savannas is well-researched in other countries and demonstrated to be helpful for suppressing woody encroachment (Wilgen *et al* 2004, Andersen *et al* 2005, Schmidt *et al* 2018).

Considering the low protection presently given to savannas, it is vital to establish protected areas that are savanna-inclusive. We located several areas in the central and eastern side of the province where savannas have persisted as candidates for potential protected areas (figure 6). While there are intact savannas that are currently unprotected, such as in central and southeast Yunnan, there are PRKs in the north that would benefit from the expansion of adjacent or nearby existing protected area boundaries.

Finally, a study that looked at how land cover change is tied up with ecosystem service values (ESVs) in northeast Yunnan stated that increasing grassland proportion with respect to forestland would increase ESVs in certain counties (Wang *et al* 2018), which underscores the contributions of savannas and forests for human well-being and biodiversity conservation. A Yunnan-wide assessment of ESVs is recommended, for understanding potential synergies and trade-offs among multiple ecosystem services in savannas and other land cover types can help improve conservation priorities (Eastburn *et al* 2017), as well as land and fire management strategies that may encourage the participation of communities as stewards of savannas (Sangha *et al* 2021).

## Data availability statement

All data that support the findings of this study are included within the article (and any supplementary files).

## Acknowledgments

This research was supported by a joint Natural Science Foundation of China-Yunnan Government research Grant to KWT (U1502264). RSL was supported by CAS-TWAS President's Fellowship for International Doctoral Students (Grant 2016CTF096). JDTDA was supported by an Academic Research Fund Grant (AcRF Tier 1) from the Singapore Ministry of Education.

## Author contributions

KWT, RSL and AKMJ planned and designed the project. RSL collected data and conducted the analyses, with assistance from AKMJ, KWT, SRCR, and JDTDA. RSL led the writing and all authors contributed critically to the drafts and gave final approval for publication.

## Declaration statement

The authors declare that they have no known competing financial interests or personal relationships that influence the work reported in this paper.

## ORCID iDs

R Sedricke Lapuz https://orcid.org/0000-0002-5072-2306
Angelica Kristina M Jaojoco https://orcid.org/0000-0002-1583-584X
Sheryl Rose C Reyes https://orcid.org/0000-0001-6201-1926
Jose Don T De Alban https://orcid.org/0000-0002-1671-5786
Kyle W Tomlinson https://orcid.org/0000-0003-3039-6766

## References

Allaire J J, Gandrud C, Russell K and Yetman C J 2017 Networkd3: D3 Javascript network graphs from R. R package version 0.4 (https://cran.r-project.org/web/packages/networkD3/index.html)
Alphan H 2017 Analysis of road development and associated agricultural land use change *Environ. Monit. Assess.* **190** 5
Andersen A N, Cook G D, Corbett L K, Douglas M M, Eager R W, Russell-Smith J, Setterfield S A, Williams R J and Woinarski J C Z 2005 Fire frequency and biodiversity conservation in Australian tropical savannas: implications from the Kapalga fire experiment *Austral Ecol.* **30** 155–67
Bastin J-F *et al* 2017 The extent of forest in dryland biomes *Science* **356** 635–8
Biasatti D, Wang Y, Gao F, Xu Y and Flynn L 2012 Paleoecologies and paleoclimates of late Cenozoic mammals from Southwest China: evidence from stable carbon and oxygen isotopes *J. Asian Earth Sci.* **44** 48–61
Bond W J 2019 *Open Ecosystems: Ecology and Evolution beyond the Forest Edge* (Oxford: Oxford University Press)
Bond W J, Woodward F I and Midgley G F 2005 The global distribution of ecosystems in a world without fire *New Phytol.* **165** 525–38
Bruggeman D, Meyfroidt P and Lambin E F 2016 Forest cover changes in Bhutan: revisiting the forest transition *Appl. Geogr.* **67** 49–66
Buitenwerf R, Bond W J, Stevens N and Trollope W S W 2012 Increased tree densities in South African savannas: >50 years of data suggests $CO_2$ as a driver *Glob. Chang Biol.* **18** 675–84
Buitenwerf R, Swemmer A M and Peel M J S 2011 Long-term dynamics of herbaceous vegetation structure and composition in two African savanna reserves: effects of rainfall on herbaceous vegetation *J. Appl. Ecol.* **48** 238–46
Chen C *et al* 2019 China and India lead in greening of the world through land-use management *Nat. Sustain.* **2** 122–9
Chu Y, Wee A K S, Lapuz R S and Tomlinson K W 2021 Phylogeography of two widespread $C_4$ grass species suggest that tableland and valley grassy biome in southwestern China pre-date human modification *Glob. Ecol. Conserv.* **31** e01835
Congedo L 2014 Semi-automatic classification plugin documentation
Cunningham M A and Johnson D 2019 Narrowness of habitat selection in woodland and grassland birds *Avian Conserv. Ecol.* **14** 14
De Alban J, Connette G, Oswald P and Webb E 2018 Combined Landsat and L-band SAR data improves land cover classification and change detection in dynamic tropical landscapes *Remote Sens.* **10** 306
Diallo Y, Hu G and Wen X 2009 Applications of remote sensing in land use/land cover change detection in Puer and Simao Counties, Yunnan Province *J. Am. Sci.* **5** 157–66
Eastburn D J, O'Geen A T, Tate K W and Roche L M 2017 Multiple ecosystem services in a working landscape *PLoS One* **12** e0166595
Edwards E J *et al* 2010 The origins of $C_4$ grasslands: integrating evolutionary and ecosystem science *Science* **328** 587–91
Ehleringer J R, Cerling T E and Helliker B R 1997 $C_4$ photosynthesis, atmospheric $CO_2$, and climate *Oecologia* **112** 285–99
ESRI 2011 *ArcGIS Desktop: Release 10*
Fensham R J, Fairfax R J and Ward D P 2009 Drought-induced tree death in savanna *Global Change Biol.* **15** 380–7
Fogarty D T, Roberts C P, Uden D R, Donovan V M, Allen C R, Naugle D E, Jones M O, Allred B W and Twidwell D 2020 Woody plant encroachment and the sustainability of priority conservation areas *Sustainability* **12** 8321
Fuhlendorf S D, Woodward A J W, Leslie D M and Shackford J S 2002 Multi-scale effects of habitat loss and fragmentation on lesser prairie-chicken populations of the US Southern Great Plains *Landscape Ecol.* **17** 617–28
Gislason P O, Benediktsson J A and Sveinsson J R 2006 Random forests for land cover classification *Pattern Recognit. Lett.* **27** 294–300
GRASS Development Team 2020 Geographic resources analysis support system (GRASS) software, version 7.8 *Open Source Geospatial Foundation* (https://grass.osgeo.org)
Griffith D M *et al* 2017 Comment on 'the extent of forest in dryland biomes' *Science* **358** eaao1309
Helm A, Oja T, Saar L, Takkis K, Talve T and Pärtel M 2009 Human influence lowers plant genetic diversity in communities with extinction debt *J. Ecol.* **97** 1329–36
Hesselbarth M H K, Sciaini M, With K A, Wiegand K and Nowosad J 2019 landscapemetrics: an open-source R tool to calculate landscape metrics *Ecography* **42** 1648–57
Higgins S I, Bond W J and Trollope W S W 2000 Fire, resprouting and variability: a recipe for grass–tree coexistence in savanna *J. Ecol.* **88** 213–29
Hirota M, Holmgren M, Nes E H V and Scheffer M 2011 Global resilience of tropical forest and savanna to critical transitions *Science* **334** 232–5
Hoffmann W A, Bazzaz F A, Chatterton N J, Harrison P A and Jackson R B 2000 Elevated $CO_2$ enhances resprouting of a tropical savanna tree *Oecologia* **123** 312–7
Honnay O, Adriaens D, Coart E, Jacquemyn H and Roldan-Ruiz I 2007 Genetic diversity within and between remnant populations of the endangered calcareous grassland plant Globularia bisnagarica L *Conserv. Genet.* **8** 293–303
Hou X 2001 *The Vegetation Atlas of China (1:1000000)* (Beijing: Science Press)
Jin Z 2002 *Floristic Features of Dry-Hot and Dry-Warm Valleys, Yunnan and Sichuan* (Kunming: Yunnan Science and Technology)
Jin Z and Ou X 2000 *Yuanjiang, Nujiang, Jinshajiang, Lancangjiang Vegetation of Dry-Hot Valley* (Kunming: Yunnan University)
Kgope B S, Bond W J and Midgley G F 2010 Growth responses of African savanna trees implicate atmospheric [$CO_2$] as a driver of past and current changes in savanna tree cover *Austral Ecol.* **35** 451–63

Khaing T T, Pasion B O, Lapuz R S and Tomlinson K W 2019 Determinants of composition, diversity and structure in a seasonally dry forest in Myanmar *Glob. Ecol. Conserv.* **13** e00669

Kumar D, Pfeiffer M, Gaillard C, Langan L, Martens C and Scheiter S 2020 Misinterpretation of Asian savannas as degraded forest can mislead management and conservation policy under climate change *Biol. Conserv.* **241** 108293

Lehmann C E R, Prior L D and Bowman D M J S 2009 Fire controls population structure in four dominant tree species in a tropical savanna *Oecologia* **161** 505–15

Liang J, Liu Y, Ying L, Li P, Xu Y and Shen Z 2014 Road impacts on spatial patterns of land use and landscape fragmentation in three parallel rivers region, Yunnan Province, China *Chin. Geogr. Sci.* **24** 15–27

Liu J *et al* 2010 Spatial patterns and driving forces of land use change in China during the early 21st century *J. Geogr. Sci.* **20** 483–94

Liu J *et al* 2014b Spatiotemporal characteristics, patterns, and causes of land-use changes in China since the late 1980s *J. Geogr. Sci.* **24** 195–210

Liu J, Liu M, Zhuang D, Zhang Z and Deng X 2003 Study on spatial pattern of land-use change in China during 1995–2000 *Sci. China* **46** 15

Liu J, Yunhong T and Slik J W F 2014a Topography related habitat associations of tree species traits, composition and diversity in a Chinese tropical forest *For. Ecol. Manage.* **330** 75–81

Liu S, Dong Y, Cheng F, Zhang Y, Hou X, Dong S and Coxixo A 2017 Effects of road network on Asian elephant habitat and connectivity between the nature reserves in Xishuangbanna, Southwest China *J. Nat. Conserv.* **38** 11–20

Liu W, Hughes A C, Bai Y, Li Z, Mei C and Ma Y 2020 Using landscape connectivity tools to identify conservation priorities in forested areas and potential restoration priorities in rubber plantation in Xishuangbanna, Southwest China *Landscape Ecol.* **35** 389–402

Loveland T R and Dwyer J L 2012 Landsat: building a strong future *Remote Sens. Environ.* **122** 22–29

Lu N, Hernandez A J and Ramsey R D 2015 Land cover dynamics monitoring with Landsat data in Kunming, China: a cost-effective sampling and modelling scheme using Google Earth imagery and random forests *Geocarto Int.* **30** 186–201

Nguyen T T, Murphy B P and Baker P J 2019 The existence of a fire-mediated tree-recruitment bottleneck in an Asian savanna *J. Biogeogr.* **46** 745–56

Ning J *et al* 2018 Spatiotemporal patterns and characteristics of land-use change in China during 2010–2015 *J. Geogr. Sci.* **28** 547–62

Olofsson P, Foody G M, Herold M, Stehman S V, Woodcock C E and Wulder M A 2014 Good practices for estimating area and assessing accuracy of land change *Remote Sens. Environ.* **148** 42–57

Olofsson P, Foody G M, Stehman S V and Woodcock C E 2013 Making better use of accuracy data in land change studies: estimating accuracy and area and quantifying uncertainty using stratified estimation *Remote Sens. Environ.* **129** 122–31

Osborne C P, Salomaa A, Kluyver T A, Visser V, Kellogg E A, Morrone O, Vorontsova M S, Clayton W D and Simpson D A 2014 A global database of $C_4$ photosynthesis in grasses *New Phytol.* **204** 441–6

Panthi S, Fan Z, Sleen P and Zuidema P A 2020 Long-term physiological and growth responses of Himalayan fir to environmental change are mediated by mean climate *Glob. Change Biol.* **26** 1778–94

Price J C 1981 The contribution of thermal data in Landsat multispectral classification *Photogramm. Eng.* **47** 229–36

R Core Team 2021 R: a language and environment for statistical computing

Ratnam J, Chengappa S K, Machado S J, Nataraj N, Osuri A M and Sankaran M 2019 Functional traits of trees from dry deciduous 'forests' of southern India suggest seasonal drought and fire are important drivers *Front. Ecol. Evol.* **7** 8

Ratnam J, Tomlinson K W, Rasquinha D N and Sankaran M 2016 Savannahs of Asia: antiquity, biogeography, and an uncertain future *Phil. Trans. R. Soc.* B **371** 20150305

Ripley B, Visser V, Christin P-A, Archibald S, Martin T and Osborne C 2015 Fire ecology of $C_3$ and $C_4$ grasses depends on evolutionary history and frequency of burning but not photosynthetic type *Ecology* **96** 2679–91

Rodriguez-Galiano V F, Ghimire B, Rogan J, Chica-Olmo M and Rigol-Sanchez J P 2012 An assessment of the effectiveness of a random forest classifier for land-cover classification *ISPRS J. Photogramm. Remote Sens.* **67** 93–104

Running S W, Loveland T R, Pierce L L, Nemani R R and Hunt E R 1995 A remote sensing based vegetation classification logic for global land cover analysis *Remote Sens. Environ.* **51** 39–48

Sangha K K, Evans J, Edwards A, Russell-Smith J, Fisher R, Yates C and Costanza R 2021 Assessing the value of ecosystem services delivered by prescribed fire management in Australian tropical savannas *Ecosyst. Serv.* **51** 101343

Sankaran M, Augustine D J and Ratnam J 2013 Native ungulates of diverse body sizes collectively regulate long-term woody plant demography and structure of a semi-arid savanna *J. Ecol.* **101** 1389–99

Scheiter S, Kumar D, Corlett R T, Gaillard C, Langan L, Lapuz R S, Martens C, Pfeiffer M and Tomlinson K W 2020 Climate change promotes transitions to tall evergreen vegetation in tropical Asia *Global Change Biol.* **26** 5106–24

Schmidt I B, Moura L C, Ferreira M C, Eloy L, Sampaio A B, Dias P A and Berlinck C N 2018 Fire management in the Brazilian savanna: first steps and the way forward *J. Appl. Ecol.* **55** 2094–101

Scholes R J and Archer S R 1997 Tree-grass interactions in savannas *Annu. Rev. Ecol. Syst.* **28** 517–44

Shen G, Gao X, Gao B and Granger D E 2009 Age of Zhoukoudian Homo erectus determined with 26Al/10Be burial dating *Nature* **458** 198–200

Shi H and Chen J 2018 Characteristics of climate change and its relationship with land use/cover change in Yunnan Province, China *Int. J. Climatol.* **38** 2520–37

Shi Z, Sha Y and Liu X 2017 Effect of Yunnan–Guizhou topography at the Southeastern Tibetan Plateau on the Indian monsoon *J. Clim.* **30** 1259–72

Simon M F, Grether R, Queiroz L P, de Skema C, Pennington R T and Hughes C E 2009 Recent assembly of the Cerrado, a neotropical plant diversity hotspot, by *in situ* evolution of adaptations to fire *PNAS* **106** 20359–64

Staver A C, Archibald S and Levin S A 2011 The global extent and determinants of savanna and forest as alternative biome states *Science* **334** 230–2

Stoffel M A, Nakagawa S and Schielzeth H 2021 partR2: partitioning R2 in generalized linear mixed models bioRxiv 2020.07.26.221168 (https://doi.org/10.1101/2020.07.26.221168)

Su Y *et al* 2020 An updated vegetation map of China (1:1000000) *Sci. Bull.* **65** 1125–36

Wang Y, Dai E, Yin L and Ma L 2018 Land use/land cover change and the effects on ecosystem services in the Hengduan Mountain region, China *Ecosyst. Serv.* **34** 55–67

Welker C A D, McKain M R, Estep M C, Pasquet R S, Chipabika G, Pallangyo B and Kellogg E A 2020 Phylogenomics enables biogeographic analysis and a new subtribal classification of Andropogoneae (Poaceae—Panicoideae) *J. Syst. Evol.* **58** 1003–30

Wilgen B W V, Govender N, Biggs H C, Ntsala D and Funda X N 2004 Response of savanna fire regimes to changing fire-management policies in a large African National park *Conserv. Biol.* **18** 1533–40

Williams A P, Allen C D, Millar C I, Swetnam T W, Michaelsen J, Still C J and Leavitt S W 2010 Forest responses to increasing aridity and warmth in the southwestern United States *Proc. Natl Acad. Sci.* **107** 21289–94

Wu G, Gao Y, Wang Y, Wang Y and Xu D 2015 Land-use/land cover changes and their driving forces around wetlands in

Shangri-La County, Yunnan Province, China *Int. J. Sustain. Dev. World Ecol.* **22** 110–6
Xu J, Ai X and Deng X 2005 Exploring the spatial and temporal dynamics of land use in Xizhuang watershed of Yunnan, southwest China *Int. J. Appl. Earth Obs. Geoinf.* **7** 299–309
Xu J, Yang Y, Fox J and Yang X 2007 Forest transition, its causes and environmental consequences: empirical evidence from Yunnan of Southwest China *Tropical Ecol.* **48** 137–50
Yao Y-F, Bruch A A, Cheng Y-M, Mosbrugger V, Wang Y-F and Li C-S 2012 Monsoon versus uplift in Southwestern China–Late Pliocene climate in Yuanmou Basin, Yunnan *PLoS One* **7** e37760
Yi K, Bao Y and Zhang J 2017 Spatial distribution and temporal variability of open fire in China *Int. J. Wildland Fire* **26** 122
Zhang J-Q, Corlett R T and Zhai D 2019a After the rubber boom: good news and bad news for biodiversity in Xishuangbanna, Yunnan, China *Reg. Environ. Change* **19** 1713–24
Zhang T-C, Comes H P and Sun H 2011 Chloroplast phylogeography of Terminalia franchetii (Combretaceae) from the eastern Sino-Himalayan region and its correlation with historical river capture events *Mol. Phylogenetics Evol.* **60** 1–12
Zhang Z, Wang B, Buyantuev A, He X, Gao W, Wang Y and Yang Z 2019b Urban agglomeration of Kunming and Yuxi cities in Yunnan, China: the relative importance of government policy drivers and environmental constraints *Landscape Ecol.* **34** 663–79
Zhao H *et al* 2019a Individual-level performance of nature reserves in forest protection and the effects of management level and establishment age *Biol. Conserv.* **233** 23–30
Zhao X, Ren B, Li D, Xiang Z, Garber P A and Li M 2019b Effects of habitat fragmentation and human disturbance on the population dynamics of the Yunnan snub-nosed monkey from 1994 to 2016 *Peer J.* **7** e6633
Zhao Y, Zhang K, Fu Y and Zhang H 2012 Examining land-use/land-cover change in the lake dianchi watershed of the Yunnan-Guizhou Plateau of Southwest China with remote sensing and GIS techniques: 1974–2008 *Int. J. Environ. Res. Public Health* **9** 3843–65
Zhu H, Tan Y, Yan L and Liu F 2020 Flora of the savanna-like vegetation in hot dry valleys, Southwestern China with Implications to their origin and evolution *Bot. Rev.* **86** 281–97